



DSC-PWI presurgical differentiation of grade 4 astrocytoma and glioblastoma in young adults: rCBV percentile analysis across enhancing and non-enhancing regions

Albert Pons-Escoda^{1,2,3} · Pablo Naval-Baudin^{1,3,4} · Mildred Viveros¹ · Susanie Flores-Casaperalta¹ · Ignacio Martínez-Zalacáin^{1,4} · Gerard Plans^{2,5} · Noemi Vidal^{2,6} · Monica Cos¹ · Carles Majos^{1,2}

Received: 14 December 2023 / Accepted: 29 May 2024 / Published online: 5 June 2024
© The Author(s) 2024

Abstract

Purpose The presurgical discrimination of IDH-mutant astrocytoma grade 4 from IDH-wildtype glioblastoma is crucial for patient management, especially in younger adults, aiding in prognostic assessment, guiding molecular diagnostics and surgical planning, and identifying candidates for IDH-targeted trials. Despite its potential, the full capabilities of DSC-PWI remain underexplored. This research evaluates the differentiation ability of relative-cerebral-blood-volume (rCBV) percentile values for the enhancing and non-enhancing tumor regions compared to the more commonly used mean or maximum preselected rCBV values.

Methods This retrospective study, spanning 2016–2023, included patients under 55 years (age threshold based on World Health Organization recommendations) with grade 4 astrocytic tumors and known IDH status, who underwent presurgical MR with DSC-PWI. Enhancing and non-enhancing regions were 3D-segmented to calculate voxel-level rCBV, deriving mean, maximum, and percentile values. Statistical analyses were conducted using the Mann-Whitney U test and AUC-ROC.

Results The cohort consisted of 59 patients (mean age 46; 34 male): 11 astrocytoma-4 and 48 glioblastoma. While glioblastoma showed higher rCBV in enhancing regions, the differences were not significant. However, non-enhancing astrocytoma-4 regions displayed notably higher rCBV, particularly in lower percentiles. The 30th rCBV percentile for non-enhancing regions was 0.705 in astrocytoma-4, compared to 0.458 in glioblastoma ($p=0.001$, AUC-ROC = 0.811), outperforming standard mean and maximum values.

Conclusion Employing an automated percentile-based approach for rCBV selection enhances differentiation capabilities, with non-enhancing regions providing more insightful data. Elevated rCBV in lower percentiles of non-enhancing astrocytoma-4 is the most distinguishable characteristic and may indicate lowly vascularized infiltrated edema, contrasting with glioblastoma's pure edema.

Keywords Brain neoplasms · Astrocytoma · Glioblastoma · Perfusion imaging · Magnetic resonance imaging

✉ Albert Pons-Escoda
albert.pons@bellvitgehospital.cat

¹ Radiology Department, Hospital Universitari de Bellvitge, Barcelona, Spain

² Neuro-oncology Unit, Institut d'Investigació Biomèdica de Bellvitge- IDIBELL, Barcelona, Spain

³ Facultat de Medicina i Ciències de La Salut, Universitat de Barcelona (UB), Barcelona, Spain

⁴ Diagnostic Imaging and Nuclear Medicine Research Group, Institut d'Investigació Biomèdica de Bellvitge- IDIBELL, Barcelona, Spain

⁵ Neurosurgery Department, Hospital Universitari de Bellvitge, Barcelona, Spain

⁶ Pathology Department, Hospital Universitari de Bellvitge, Barcelona, Spain

Abbreviations

DSC-PWI	Dynamic-Susceptibility-Contrast Perfusion-Weighted-Imaging
rCBV	Relative Cerebral Blood Volume
IDH	Isocitrate Dehydrogenase
WHO	World Health Organization
ROI	Region Of Interest
AUC-ROC	Area Under the Receiver Operating Characteristic Curve

Introduction

According to the latest World Health Organization (WHO) classification of CNS tumors, Isocitrate Dehydrogenase (IDH)-mutant astrocytoma grade 4 is no longer referred to as Glioblastoma. This term is now reserved exclusively for IDH-wildtype grade 4 astrocytic tumors [1]. A non-invasive differentiation of these grade 4 astrocytic tumors could have significant implications for patient management [2–7]. Astrocytoma grade 4 has been less extensively studied compared to its grade 2–3 counterparts, remaining a major radiological challenge. While lower-grade IDH-mutant astrocytomas typically appear as non-enhancing and non-necrotic on morphological images, grade 4 astrocytomas can mimic the imaging characteristics of glioblastomas. Both often exhibit enhancement and necrosis, contrasting starkly with their grade 2–3 IDH-mutant counterparts [7–13]. This overlap in morphological features between IDH-mutant and IDH-wildtype grade 4 tumors highlights the need for advanced quantitative MR techniques, such as Dynamic-Susceptibility-Contrast Perfusion-Weighted-Imaging (DSC-PWI).

DSC-PWI provides insights into the tumors' vascular and microvascular environments [14], particularly relevant because microvascular proliferation is a defining feature of grade 4 according to the 2021 WHO classification [1]. As a result, predictably, both of these tumors, regardless of IDH status, should exhibit elevated relative cerebral-blood-volume (rCBV), which can be considered a radiological manifestation of microvascular proliferation. Thus, the question arises: Does high rCBV predict IDH-mutation status or merely denote a grade 4 tumor? Traditionally, rCBV calculations have focused on either mean or extreme values (maximum or “hot-spots”) derived from manually delineated regions-of-interest (ROIs) or entire tumor volumetric segmentations. The practice of using preselected single rCBV values, particularly when focused solely on specific ROIs, tends to overlook tumor heterogeneity, potentially overlooking significant differences across the entire tumor and spectrum of rCBV values [15, 16]. Furthermore, in these grade 4 tumors, both enhancing and non-enhancing

components often coexist, which represent different tumor environments, and their separate evaluation could offer diverse perspectives [17].

Differentiating astrocytoma grade 4 and glioblastoma is especially crucial in patients under 55-year-old. According to WHO guidelines, DNA sequencing to confirm IDH mutation status in grade 4 astrocytic tumors is mandatory for patients under 55 years of age, while negative immunohistochemistry suffices for those above this age, given the rarity of IDH mutations beyond this threshold. Yet, for those under 55, IDH mutations are more balanced, emphasizing the need for accurate differentiation in this age group [1, 7, 18, 19]. Given the heavily correlated factors of age, grade, and IDH-mutation status, studies must approach these entities with care to ensure accurate representation of data and interpretation. Thus, focused studies are crucial for a deeper understanding.

Based on these rationales, we believe that the pre-surgical differentiation between IDH-mutant astrocytoma grade 4 and IDH-Wildtype Glioblastoma deserves specific attention [13]. The primary objective of this work is to study the potential of rCBV in distinguishing the IDH-mutation status of grade 4 astrocytic tumors in an age-adjusted cohort, in accordance with WHO recommendations regarding IDH-mutations [1, 18, 19]. We aim to assess both the enhancing and non-enhancing components in a comprehensive voxel-wise, automated, unsupervised manner (exploratory, without the input of prior knowledge or assumptions) using histogram-derived percentile values, contrasting with conventional methods that rely on preselected rCBV values such as mean or maximum.

Methods

This retrospective study received approval from the Research Ethics Committee of our tertiary hospital.

Patients

Patients diagnosed with IDH-mutant astrocytoma grade 4 and IDH-wildtype glioblastoma were retrospectively retrieved from our centre's database spanning the years 2016–2023. The study's inclusion criteria were as follows: (1) Confirmed tumor diagnosis in accordance with the WHO Classification of CNS Tumors 2021 criteria; (2) Age under 55-year-old at the time of tumor diagnosis, adhering to the WHO recommendations; and (3) Availability of a diagnostic pre-surgical MR imaging examination that includes DSC-PWI, T1WI, T2WI, FLAIR, and contrast-enhanced T1WI (CE-T1WI). The study's exclusion criterion was the absence of any of the sequences or a low quality that

prevented adequate tumor segmentation or DSC-PWI data extraction.

Imaging

The MR imaging examinations included in the study were performed using a 1.5-T scanner (Ingenia, Philips Healthcare). All DSC-PWI sequences were gradient-echo, with the following technical parameters: Echo Time, 40ms; Repetition Time, 1500–1700ms; Flip-Angle, 75°; Pixel size, 1.75 mm; Slice Thickness, 5 mm; Image size, 128×128; Number of Slices, 20–25; Number and duration of Dynamics, 60 and 1.5s. A single dose of 0.1 mmol/kg of intravenous gadolinium-based contrast agent (1 mmol/mL) was injected at a rate of 4–5 mL/s. Baseline was in the order of 10–15 points. The quality of the sequences was assessed by two experienced neuroradiologists: A.P.-E and PN-B with more than 10 and 5 years of experience in neuroradiology. Examinations were labelled as poor quality and thus excluded from the study if: (1) motion artifacts prevented the segmentation or coregistration, or (2) an obvious low signal-to-noise ratio was visually assessable in the mean raw time-intensity curves.

Post-processing and DSC-PWI data extraction

After following the standard recommended preprocessing steps, the HD-GLIO pipeline was utilized to segment both enhancing and non-enhancing regions of the whole brain tumor-related abnormality, considering axial T1WI, T2WI, FLAIR, and CE-T1WI [20, 21]. Necrosis was excluded. Subsequently, the FAST tool within FSL was employed to acquire the segmentation for normal-appearing white matter for normalization purposes [22]. Finally, the segmentations were co-registered with the DSC-PWI using the 3D Slicer BRAINSFit module (<http://www.slicer.org>). The segmentations were reviewed and verified by two experienced neuroradiologists: A.P.-E. and PN-B. For each voxel within the tumor segmentations, normalized and leakage corrected rCBV was calculated as described by Boxerman et al. [14]. For each patient's tumor segmentations, the mean and maximum values of all the voxels as well as percentile values in increments of five were calculated.

Description and comparison of DSC-PWI metrics

Statistical comparisons were conducted for Grade 4 Astrocytoma and Glioblastoma rCBV mean, maximum and percentile values via a Mann-Whitney U test. Simultaneously, we calculated the area under the receiver operating characteristic curve (AUC-ROC) for all rCBV values. Finally,

box-plots were constructed to visually assess the segregation potential of the different rCBV value.

As an addition, just to reinforce our observations that these two tumors display similar characteristics on morphological imaging, we referred to the most recent research [8–13]. According to these studies, the primary imaging markers for IDH-mutation status on morphological MRI might include nodular enhancement, necrosis, and T2-FLAIR mismatch. These markers were assessed dichotomously (for enhanced clarity, reproducibility and robustness) by two experienced radiologists (AP-E and PN-B), who determined the presence or absence of such signs.

Results

Patients

The initial cohort consisted of 63 grade 4 astrocytic tumors in patients under 55-year-old. This group was made up of 12 Astrocytoma grade 4 (Astrocytoma 4) and 51 Glioblastoma. Four tumors (1 Astrocytoma 4, and 3 Glioblastomas) were excluded due to the absence of DSC-PWI or the presence of motion artifacts that precluded accurate tumor segmentation or DSC-PWI data extraction. Consequently, the resulting dataset comprised 59 tumors: 11 Astrocytoma 4, and 48 Glioblastoma. A flowchart detailing the patient selection process is provided in Fig. 1.

Demographic details, including age and sex, are presented in Table 1. This table also highlights statistical comparisons between the two groups. The mean age across the dataset was 46-year-old, with 34 of the 59 participants being male. Despite the age-centric nature of the study, a significant age difference ($p=0.009$) emerged between the entities, with Glioblastoma patients being slightly older, which aligns with prior knowledge [1]. Additionally, warranting particular mention and fully consistent with established knowledge, our reference centre's brain tumor database did not include any Astrocytoma 4 in patients over 55-year-old.

Regarding morphological imaging evaluation (detailed in Table 2), the T2-FLAIR mismatch was the only visual feature showing significant differences associated with IDH-mutation status, boasting perfect specificity. However, it was observed in just 27% of the cases. No significant differences were observed in the presence or absence of nodular enhancement or necrosis, present in vast majority of cases for both entities as shown in Fig. 2.

Description and comparison of DSC-PWI metrics

Tables 3 and 4 present the results for rCBV comparisons using the U-Mann Whitney p-values and AUC-ROCs for

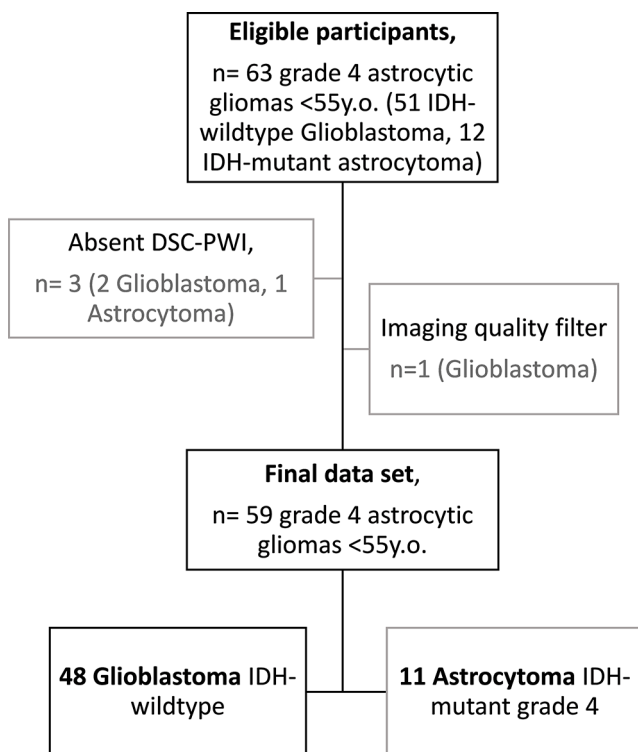


Fig. 1 A flowchart that summarizes the study participant selection process

enhancing and non-enhancing regions respectively. In the context of the enhancing tumor (Table 3), IDH-wildtype displayed higher values overall, but no significant differences emerged between the two tumor types. Interestingly, the lower percentiles (those between p5 and p35) in enhancing regions showed higher rCBV values in IDH-mutant, also no significant. For the non-enhancing regions (Table 4), all rCBV percentile values exhibited significant differences between both entities, using the conventional p-value threshold of 0.05. Overall rCBV in non-enhancing regions

were higher in Astrocytomas 4. Applying the more stringent threshold of $p < 0.005$, recently proposed as more robust [23], the mean rCBV (Astrocytoma = 1.48 vs. Glioblastoma = 1.14) and percentile rCBV values between p10 and p60 (Astrocytoma = 0.35–1.32 vs. Glioblastoma = 0.21–0.96) remain significant. In AUC-ROC analysis, excellent discriminatory power considered as above 0.8 [24], was demonstrated by the percentiles between p15 and p30. Whisker-plots for the mean and maximum rCBV of enhancing region are shown in Fig. 3. The plots for non-enhancing region mean, maximum, and the best percentile (p30) rCBV values are shown in Fig. 4. These figures allow for a visual assessment of the different discriminative capabilities and values dispersion. The sensitivity and specificity of rCBVp30, the best percentile, were 0.82 and 0.71, respectively, for a threshold of 0.56.

To clarify, for example, p5 corresponds to the rCBV value below which 5% of voxels within the segmented volume-of-interest fall, meaning 95% are above it, while p10 is the value below which 10% of voxels fall, meaning 90% are above it, and so forth. Therefore, for instance the range from p5 to p35 represents the lower range of rCBV values within the segmented volume-of-interest, from the 5th percentile to the 35th percentile, with values above the lowest 5% and below the highest 65%. For clarity and transparency, we provide the full list of results for all percentiles in both tumor regions. This approach offers an exploratory alternative without relying on prior knowledge or assumptions, and studying all percentiles ensures full data availability and the robustness of the provided information.

Two additional subanalyses were conducted to reinforce the main findings: one involved a class-balanced 5-fold internal cross-validation to address potential class imbalance (11 Astrocytoma: 48 Glioblastoma) biases, and the other applied Bonferroni corrections to p-values. These are detailed in Supplementary Materials 1 and 2, respectively.

Table 1 This table presents the demographic and clinical characteristics of the participants, including age, sex, and tumor grade

	Grade 4 astrocytoma IDH-Mutant	Glioblastoma IDH-wildtype	Whole data-set	<i>p</i> -value
Age (years), Mean +/-SD	41 +/-8	47 +/- 6	46 +/- 7	0.009*
Sex, Men: Women	6: 5	28: 20	34: 25	1
Total	11	48	59	

Statistical comparisons were made using the U-Mann Whitney Test for age, and the Chi-Square test for sex. SD denotes Standard Deviation. (*) indicates statistical significance, $p < 0.05$.

Table 2 Distribution of presence of Nodular enhancement, necrosis and T2-FLAIR mismatch among tumor groups

Tumor type/ imaging features	Grade 4 astrocytoma IDH-Mutant	Glioblastoma IDH-wildtype	<i>p</i> -value
Nodular enhancement	9/11 (82%)	47/48 (98%)	0.16
Necrosis	9/11 (82%)	44/48 (92%)	0.52
T2-FLAIR mismatch	3/11 (27%)	0/48 (0%)	0.03*

Statistical comparisons were made using Chi-Square. (*) indicates statistical significance, $p < 0.05$.

Fig. 2 Illustrative cases of patients aged between 36 and 51 years diagnosed with Astrocytoma grade 4 (A–C) and Glioblastoma (D–F). These cases demonstrate overlapping imaging characteristics on morphological MR (FLAIR and CE-T1WI) and rCBV color maps. Features such as non-enhancing regions, nodular enhancements, conspicuous signs of necrosis, and high rCBV are common to both tumor types in all shown cases

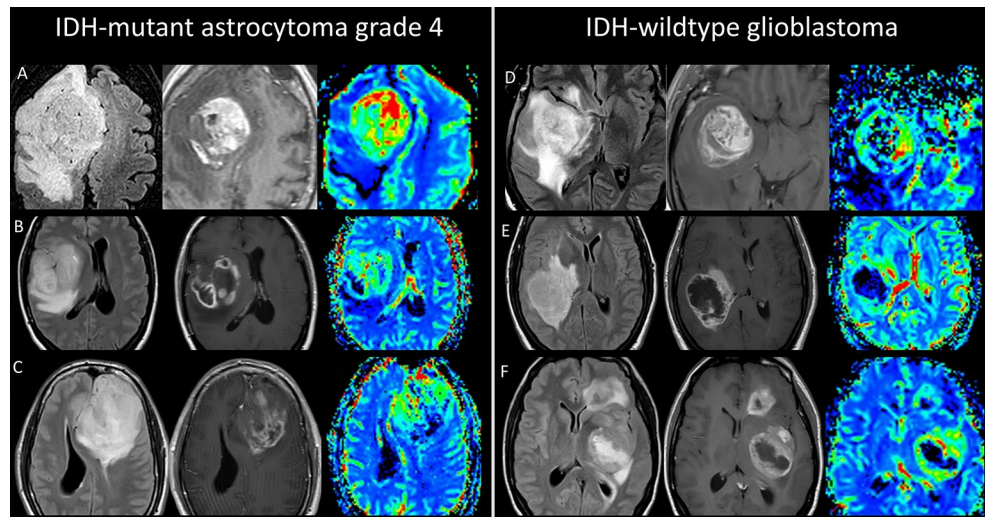


Table 3 Average rCBV values (mean, maximum, and percentiles) for both tumor types in enhancing regions

Enhancing region							
Astro 4	rCBV	Mean	Gb	rCBV	Mean	<i>p</i>	AUC-ROC
	rCBV mean	2.496		rCBV mean	2.784	0.315	0.608
	rCBV p5	0.638		rCBV p5	0.359	0.074	0.690
	rCBV p10	0.901		rCBV p10	0.648	0.103	0.674
	rCBV p15	1.074		rCBV p15	0.894	0.255	0.622
	rCBV p20	1.275		rCBV p20	1.117	0.360	0.598
	rCBV p25	1.454		rCBV p25	1.321	0.475	0.577
	rCBV p30	1.577		rCBV p30	1.513	0.672	0.546
	rCBV p35	1.715		rCBV p35	1.707	0.947	0.508
	rCBV p40	1.860		rCBV p40	1.902	1.000	0.501
	rCBV p45	2.009		rCBV p45	2.106	0.841	0.522
	rCBV p50	2.157		rCBV p50	2.322	0.672	0.546
	rCBV p55	2.300		rCBV p55	2.539	0.577	0.560
	rCBV p60	2.471		rCBV p60	2.777	0.422	0.586
	rCBV p65	2.649		rCBV p65	3.045	0.315	0.608
	rCBV p70	2.830		rCBV p70	3.337	0.237	0.626
	rCBV p75	3.043		rCBV p75	3.700	0.160	0.650
	rCBV p80	3.373		rCBV p80	4.122	0.147	0.655
	rCBV p85	3.812		rCBV p85	4.659	0.129	0.662
	rCBV p90	4.617		rCBV p90	5.417	0.141	0.657
	rCBV max	5.772		rCBV max	6.763	0.090	0.681

Statistical comparisons were conducted using the U-Mann Whitney Test and AUC-ROC. (*) indicates statistical significance, $p < 0.05$ and/or AUC-ROC > 0.8 . (**) indicates statistical significance, $p < 0.005$.

In these analyses, the lower percentiles of non-enhancing regions remained significant and exhibited stable AUC-ROC values under very stringent conditions, whereas the mean and maximum values lost their significance. This confirms our main results, highlighting not only the superior performance of lower percentiles in the non-enhancing regions but also their greater veracity, robustness and stability compared to the mean and maximum values. For additional comparison of the main rCBV variables, an additional figure of dispersion graphics is also provided in Supplementary Material 3.

Discussion

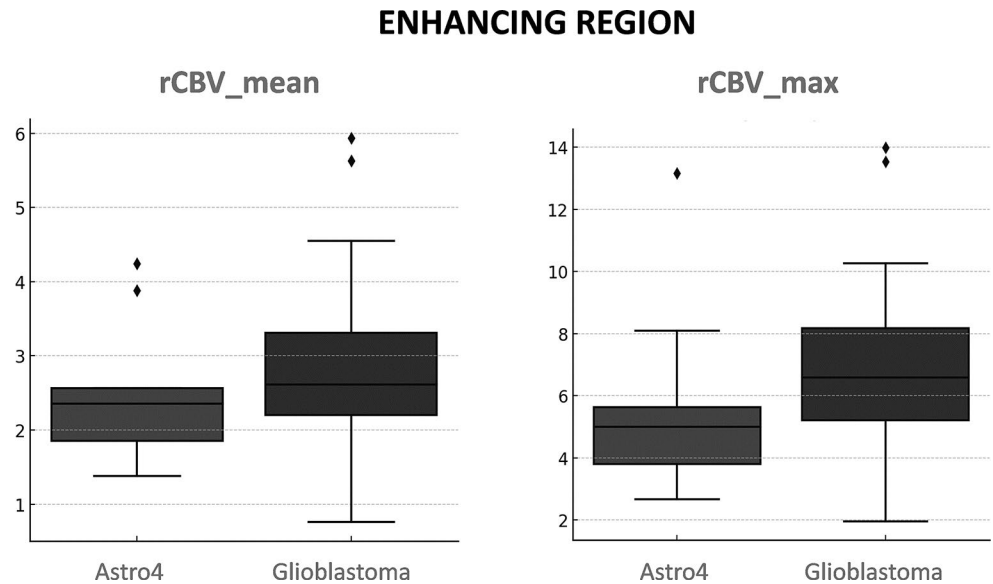
In this study, we assessed the discriminatory potential of rCBV derived from DSC-PWI to non-invasively differentiate between IDH-mutant astrocytoma grade 4 and IDH-wildtype glioblastoma pre-surgically. Our voxel-wise approach, which accounted for volumetric segmentations and all percentile values, revealed that the most discriminative rCBV values lie within the lower percentiles of the non-enhancing regions. Here, though the values are overall low, they are notably higher in IDH-mutant tumors,

Table 4 Average rCBV values (mean, maximum, and percentiles) for both tumor types in non-enhancing regions

Non-enhancing region							
Astro 4	rCBV	Mean	Gb	rCBV	Mean	<i>p</i>	AUC-ROC
	rCBV mean	1.484		rCBV mean	1.137	0.004**	0.782
	rCBV p5	0.204		rCBV p5	0.122	0.053	0.689
	rCBV p10	0.353		rCBV p10	0.205	0.003**	0.792
	rCBV p15	0.449		rCBV p15	0.270	0.002**	0.801*
	rCBV p20	0.535		rCBV p20	0.335	0.002**	0.807*
	rCBV p25	0.621		rCBV p25	0.396	0.001**	0.811*
	rCBV p30	0.705		rCBV p30	0.458	0.001**	0.811*
	rCBV p35	0.794		rCBV p35	0.526	0.002**	0.799
	rCBV p40	0.881		rCBV p40	0.590	0.002**	0.797
	rCBV p45	0.979		rCBV p45	0.662	0.003**	0.79
	rCBV p50	1.082		rCBV p50	0.745	0.002**	0.795
	rCBV p55	1.194		rCBV p55	0.846	0.003**	0.792
	rCBV p60	1.321		rCBV p60	0.957	0.004**	0.784
	rCBV p65	1.459		rCBV p65	1.084	0.006*	0.771
	rCBV p70	1.623		rCBV p70	1.236	0.008*	0.759
	rCBV p75	1.832		rCBV p75	1.420	0.008*	0.759
	rCBV p80	2.091		rCBV p80	1.652	0.015*	0.739
	rCBV p85	2.434		rCBV p85	1.972	0.020*	0.727
	rCBV p90	2.985		rCBV p90	2.498	0.022*	0.723
	rCBV max	4.080		rCBV max	3.440	0.025*	0.72

Statistical comparisons were conducted using the U-Mann Whitney Test and AUC-ROC. (*) indicates statistical significance, $p < 0.05$ and/or AUC-ROC > 0.8 . (**) indicates statistical significance, $p < 0.005$.

Fig. 3 Whisker plots depict the distribution of mean and maximum rCBV values for the enhancing region of each tumor subtype. For clarity, only mean and maximum rCBV values are shown due to their widespread utilization in clinical practice, and also because none of the percentiles yielded significantly improved results



suggesting the benefit of using an unsupervised rCBV selection approach over the conventional reliance on preselected mean or maximum values.

Furthermore, given the well-known coexistence of tumor infiltration and edema in the non-enhancing regions, we propose that these differential rCBV values may stem from varying degrees of tumor infiltration in these low-vascularized non-enhancing areas. Such regions may represent a greater degree of coexisting very-low vascularized infiltrated tissue in IDH-mutant cases, while in IDH-wildtype

cases, they may more closely align with pure edema. Indeed, this hypothesis aligns well with prior knowledge: Glioblastomas are known to generate more pronounced edema, whereas Astrocytomas manifest a more substantial proportion of non-enhancing tumor tissue in the T2-FLAIR abnormality [25].

The observed elevated rCBV values in enhancing regions in both tumors, with no significant differences between them, would support the hypothesis that microvascular proliferation is a characteristic of grade 4 tumors, rather than

NON- ENHANCING REGION

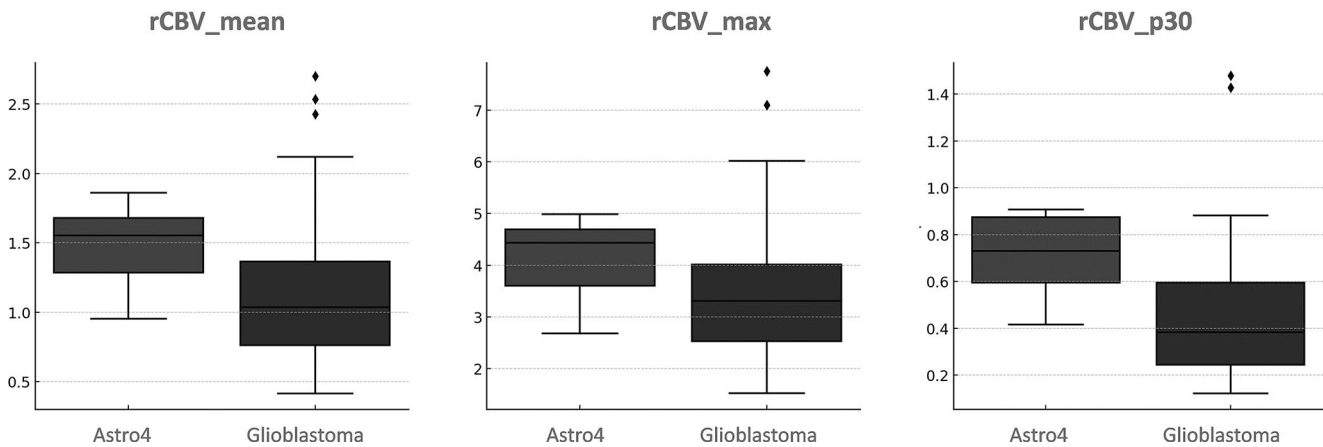


Fig. 4 Whisker plots display the distribution of mean, maximum, and best percentile (p30) rCBV values for the non-enhancing region of each tumor subtype. For clarity, mean and maximum rCBV values are shown for comparison purposes because they are the most standard

measures used in clinical practice. Meanwhile, p30 represents the best percentile result and surpasses those obtained with the standard approaches

a specific attribute of IDH-mutation status. Interestingly, the lower percentile rCBV values for Astrocytoma grade 4 tend to be slightly higher than those for Glioblastoma within these enhancing regions. This trend may suggest a higher homogeneity in Astrocytomas, characterized by a narrower range of rCBV values when compared to Glioblastomas.

Grade 4 Astrocytomas present morphological imaging traits that are distinct from grade 2–3 but are more reminiscent of IDH-wildtype Glioblastoma. The challenge of radiologically distinguishing between these two entities is highlighted by the morphological evaluations in this study, as illustrated in Fig. 2; Table 2, when considering the main markers described for differentiating between IDH-mutant and IDH-wildtype tumors [8–13].

Additionally, this study underscores the clinical significance of this differentiation in patients under 55 years old. In realistic clinical settings, the differentiation becomes crucial in this age group, making our findings especially pertinent. Unlike in those over 55 where the prevalence of the IDH mutation is negligible [1, 18, 19]. This approach mirrors a real-world clinical scenario where such differentiation is genuinely pertinent and impactful. For instance, the non-invasive presurgical differentiation of grade 4 astrocytic tumors is relevant beyond the ultimate histopathological diagnosis and could profoundly impact patient management across different levels. First, in specific scenarios, it could influence surgical decisions, such as whether to opt for function-preserving surgery or a biopsy (in cases of suspected grade 4 astrocytomas) versus total resection (in cases of suspected glioblastomas), particularly in challenging locations. Second, it may guide the sequence of the diagnostic workflow in histopathology and molecular pathology. For

instance, by emphasizing and optimizing DNA sequencing utilization (often costly or difficult to access) in the most indicated cases to optimally detect IDH mutations. Ultimately, it offers an early prognosis prediction, which is invaluable, especially for young adults, and their families, enabling informed decisions and setting realistic expectations. Furthermore, such differentiation could be instrumental for the early detection of clinical trial candidates, for instance, for trials on treatments targeting IDH, which are anticipated to increase due to recent positive outcomes [2]. As we move further into the era of personalized and targeted therapies, the insights from our study could play an increasingly important role in shaping treatment strategies. This, in turn, hopefully will positively influence the disease course and enhance the quality of life for patients [3–6]. An illustrative example of potential clinical applicability of results in new patients with unknown diagnosis is shown in Fig. 5. Four additional illustrative cases are provided in Supplementary Material 4, along with the rCBVp30 values for the entire dataset.

Several studies have attempted to identify IDH-mutation status using rCBV while analysing a range of adult diffuse gliomas. Some suggest the feasibility of discerning IDH mutation status, generally reporting higher rCBV values in both enhancing and non-enhancing regions for IDH-wildtype [17, 26, 27]. However, interpreting these findings requires caution, as these studies do not account for potential confounding with age or histological grade which are only reported as descriptive statistics, thereby preventing the optimal discernment of the specific differential in the current study. As an exemplification, considering that the vast majority of grade 4 astrocytic tumors are indeed

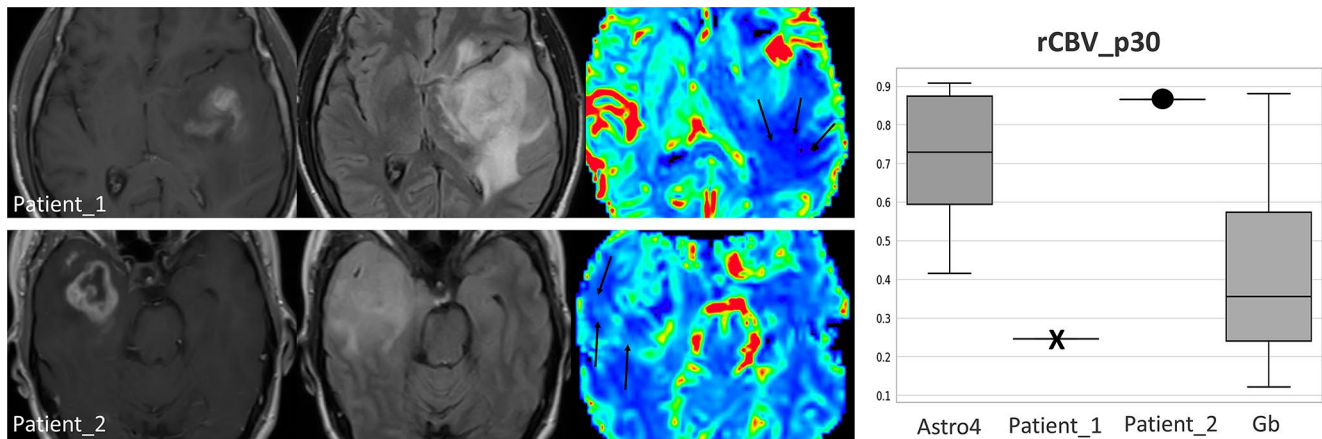


Fig. 5 Illustrative cases of two patients with unknown diagnosis: Patient_1 is 51 years old, and Patient_2 is 49 years old. The images display an extensive non-enhancing component beyond the enhancing tumor margins. This could be attributed to infiltrative tumor, edema, or a coexistence of both. rCBV color maps focused analysis allow the detection of small foci of slightly elevated rCBV (arrows) in the

glioblastomas, and the vast majority of grade 2–3 are IDH-mutant astrocytomas, a study claiming to identify IDH mutation status might actually be reflecting a more familiar differentiation between grade 2–3 and grade 4. Lastly, it is crucial to recognize that astrocytoma grade 4 is often either absent or significantly underrepresented in such studies, which limits the applicability of their results to this specific, smaller subgroup. This subgroup necessitates particular attention, as provided in our study.

Our literature search yielded only two DSC-PWI studies explicitly focused on grade 4 astrocytic tumors [28, 29], which in general terms reported higher rCBV values in IDH-wildtype tumors. However, due to different methodological approaches, direct comparison of results is not feasible. We consider relevant strengths of our methodology to include volumetric segmentations of easily demarcated morphological MR main tumor regions, which provide information on the entire abnormality; and the comprehensive evaluation of voxel-wise rCBV values through percentile analysis, not limited to preselected mean or maximum, which may obscure relevant differences in other parts of the full range of values.

Finally, another advanced MR technique deserving mention in this scenario is MR spectroscopy. It has been proven useful for IDH-mutation identification through specifically edited sequences, achieving high accuracies [30]. Also, more standard MR spectroscopy protocols offer information for glioma classification under the latest WHO guidelines [31]. However, the specific focused performance in grade 4 astrocytic tumors remains less clear because existing research again mixes tumor grades 2, 3, and 4. A potential limitation of this technique is its less extended implementation and use in neuroradiology departments worldwide compared to the

non-enhancing component of Patient_2, while it depicts clear areas of very low rCBV (arrows) in Patient_1. Quantification of the 30th percentile in non-enhancing areas indicates that Patient_1 has values that fall within the range of Glioblastoma (Gb), while Patient_2 aligns with Astrocytoma grade 4 (Astro 4). The diagnoses for both cases were histopathology confirmed

widely extended and accepted DSC-PWI for brain tumor imaging [14, 15, 32, 33]. At any instance, recognizing the challenges, we believe that an ideal approach for the near future would combine comprehensive imaging data, including DSC-PWI and MR spectroscopy, with advanced data analysis techniques, such as AI and radiomics, to enhance presurgical tumor classification.

This study comes with several limitations. This is a single-site retrospective investigation. Nevertheless, this approach ensured data homogeneity, useful in pilot studies. The sample size, though seeming modest, is justified as all tumors were classified based on the stringent 2021 WHO Classification criteria, limiting retrospective patient inclusion. Also, IDH-mutant grade 4 astrocytomas are infrequent tumors, and they are rarely addressed in recent literature as a separate entity from their grade 2–3 counterparts. We recognize that theoretically, preloaded or low Flip-Angle (30°) DSC-PWI sequences might optimize rCBV measures when aligned with histological vascularization evaluations [14]. Yet, the primary differences lie in the non-enhancing region of tumors, where leakage-effects due to blood-brain-barrier disruption should be negligible, thus reducing the impact on rCBV calculations. Moreover, our study's main focus wasn't solely on this alignment. Different techniques have also shown reproducibility and robustness and we applied rigorous leakage correction procedures, mitigating potential leakage impacts [34]. Additionally, it should be highlighted that many clinicians have a preference for non-preloaded intermediate-high Flip-Angle sequences, particularly when it comes to the pre-surgical differential diagnosis [35–41]. This preference aligns with our study's context and has demonstrated to be useful for diffuse gliomas' genetic subtypes presurgical differentiation [42, 43].

However, our methodology can adapt to different DSC-PWI techniques with simple threshold adjustments [44]. Nevertheless, broader multicentric validations remain essential. Lastly, unfortunately, analysing a single case using our proposed methodology currently requires 10–15 min, hindered by the limitations of commercial software in PACS systems that force the use of multiple tools. This situation could impede rapid clinical adoption, but also highlights an opportunity for software enhancement in clinical neuroradiology, especially through improved segmentation tools and presenting CBV values via percentile analysis. With these improvements, post-processing time could potentially be reduced to around 2 min, underscoring the need for software advancements to narrow the gap between clinical practice and research in neuroradiology.

On the other hand, our study's strengths are evident. All tumors were rigorously classified as per the 2021 WHO Classification criteria, ensuring contemporaneity. The tumor groups have been carefully balanced accounting for grade and age. Our insights hold clinical relevance from multiple discussed vantage points. Notably, the automatization of the data-extraction and data-selection ensures reproducibility minimizing operator-dependency. We underscore the importance of an unsupervised evaluation of the tumors' entire percentile values, challenging the common clinical practice of relying on ROIs, mean or maximum values. In essence, our findings could be extrapolated to other clinical scenarios, laying the groundwork for further research.

Conclusion

Using an unsupervised percentile-based approach to select rCBV values from volumetric segmentations provides richer information compared to the use of ROIs and preselected mean and maximum values.

The non-enhancing components of grade 4 astrocytic tumors are potentially more informative than the enhancing region itself.

Although globally low, higher rCBV values in the lower percentiles of the non-enhancing region in IDH-mutant grade 4 astrocytomas rose as the most distinguishing feature from glioblastomas. This suggests that different proportions of infiltrative versus vasogenic edema might be a clue for differentiating these two tumor types.

Supplementary Information The online version contains supplementary material available at <https://doi.org/10.1007/s00234-024-03385-0>.

Acknowledgements Albert Pons-Escoda and Carles Majos acknowledge support from the Instituto de Salud Carlos III (Proyectos de Investigación en Salud, PI20/00360). The authors thank CERCA Programme/Generalitat de Catalunya for institutional support.

Author contributions Albert Pons-Escoda created the experimental design. Albert Pons-Escoda led the investigation. Albert Pons-Escoda, Noemi Vidal and Carles Majos did the data collection. Albert Pons-Escoda and Pablo Naval-Baudin led the imaging-data processing and extraction. Albert Pons-Escoda, Pablo Naval-Baudin and Ignacio Martinez-Zalacain performed the statistical data analysis. Albert Pons-Escoda wrote up the manuscript and chose the best tables and figures. Albert Pons-Escoda did the bibliographic research. Pablo Naval-Baudin, Ignacio Martinez-Zalacain and Carles Majos made important contributions to the final manuscript. Monica Cos and Carles Majos offered relevant logistic support. All the authors played a role in any of the necessary patient data acquisition. All the authors have participated in the review, and correction of the manuscript. All the authors have read and approved its submission to this journal.

Funding No funding was received to assist with the preparation of this manuscript.

Open Access funding provided thanks to the CRUE-CSIC agreement with Springer Nature.

Declarations

Ethical approval and informed consent Institutional Review Board approval was obtained. Written informed consent was waived by the Institutional Review Board.

Conflict of interest The authors declare that we have no conflict of interest to disclose.

Open Access This article is licensed under a Creative Commons Attribution 4.0 International License, which permits use, sharing, adaptation, distribution and reproduction in any medium or format, as long as you give appropriate credit to the original author(s) and the source, provide a link to the Creative Commons licence, and indicate if changes were made. The images or other third party material in this article are included in the article's Creative Commons licence, unless indicated otherwise in a credit line to the material. If material is not included in the article's Creative Commons licence and your intended use is not permitted by statutory regulation or exceeds the permitted use, you will need to obtain permission directly from the copyright holder. To view a copy of this licence, visit <http://creativecommons.org/licenses/by/4.0/>.

References

1. WHO Classification of Tumours Editorial Board Central nervous system tumours [Internet] Lyon (France): International Agency for Research on Cancer; 2021 [cited 2023 Jul 13]. (WHO classification of tumours series, 5th ed.). <https://tumourclassification.iarc.who.int/chapters/45>
2. Mellinghoff IK, van den Bent MJ, Blumenthal DT et al (2023) Vorasidenib in IDH1- or IDH2-Mutant low-Grade Glioma. *N Engl J Med*. <https://doi.org/10.1056/NEJMoa2304194>
3. Mitchell D, Shireman JM, Dey M (2022) Surgical Neuro-Oncology. *Neurol Clin* 40:437–453. <https://doi.org/10.1016/j.ncl.2021.11.003>
4. Balana C, Castañer S, Carrato C et al (2022) Preoperative diagnosis and molecular characterization of Gliomas with Liquid Biopsy and Radiogenomics. *Front Neurol* 13:865171. <https://doi.org/10.3389/fneur.2022.865171>
5. Vagvala S, Guenette JP, Jaimes C, Huang RY (2022) Imaging diagnosis and treatment selection for brain tumors in the era

- of molecular therapeutics. *Cancer Imaging* 22:19. <https://doi.org/10.1186/s40644-022-00455-5>
6. Blobner J, Dengler L, Blobner S et al (2023) Significance of molecular diagnostics for therapeutic decision-making in recurrent glioma. *Neuro-Oncology Adv* 5:vdad060. <https://doi.org/10.1093/nojnl/vdad060>
 7. Pons-Escoda A, Majos C, Smits M, Oleaga L (2024) Presurgical diagnosis of diffuse gliomas in adults: Post-WHO 2021 practical perspectives from radiologists in neuro-oncology units. *Radiol (English Ed)*. <https://doi.org/10.1016/j.rxeng.2024.03.002>.
 8. Kamble AN, Agrawal NK, Koundal S et al (2023) Imaging-based stratification of adult gliomas prognosticates survival and correlates with the 2021 WHO classification. *Neuroradiology* 65:41–54. <https://doi.org/10.1007/s00234-022-03015-7>
 9. Joyner DA, Garrett J, Batchala PP et al (2023) MRI features predict tumor grade in isocitrate dehydrogenase (IDH)-mutant astrocytoma and oligodendroglioma. *Neuroradiology* 65:121–129. <https://doi.org/10.1007/s00234-022-03038-0>
 10. Lasocki A, Buckland ME, Molinaro T et al (2023) Correlating MRI features with additional genetic markers and patient survival in histological grade 2–3 IDH-mutant astrocytomas. *Neuroradiology* 65:1215–1223. <https://doi.org/10.1007/s00234-023-03175-0>
 11. Lasocki A, Buckland ME, Drummond KJ et al (2022) Conventional MRI features can predict the molecular subtype of adult grade 2–3 intracranial diffuse gliomas. *Neuroradiology* 64:2295–2305. <https://doi.org/10.1007/s00234-022-02975-0>
 12. Park YW, Han K, Ahn SS et al (2018) Prediction of IDH1 -Mutation and 1p/19q-Codeletion status using preoperative MR Imaging Phenotypes in Lower Grade Gliomas. *Am J Neuroradiol* 39:37–42. <https://doi.org/10.3174/ajnr.A5421>
 13. Lee MD, Patel SH, Mohan S et al (2023) Association of partial T2-FLAIR mismatch sign and isocitrate dehydrogenase mutation in WHO grade 4 gliomas: results from the ReSPOND consortium. *Neuroradiology* 65:1343–1352. <https://doi.org/10.1007/s00234-023-03196-9>
 14. Boxerman JL, Quarles CC, Hu LS et al (2020) Consensus recommendations for a dynamic susceptibility contrast MRI protocol for use in high-grade gliomas. *Neuro Oncol* 22:1262–1275. <https://doi.org/10.1093/neuonc/noaa141>
 15. Pons-Escoda A, Smits M (2023) Dynamic-susceptibility-contrast perfusion-weighted-imaging (DSC-PWI) in brain tumors: a brief up-to-date overview for clinical neuroradiologists. *Eur Radiol*. <https://doi.org/10.1007/s00330-023-09729-3>
 16. Pons-Escoda A, Garcia-Ruiz A, Naval-Baudin P et al (2022) Voxel-level analysis of normalized DSC-PWI time-intensity curves: a potential generalizable approach and its proof of concept in discriminating glioblastoma and metastasis. *Eur Radiol*. <https://doi.org/10.1007/s00330-021-08498-1>
 17. Wu H, Tong H, Du X et al (2020) Vascular habitat analysis based on dynamic susceptibility contrast perfusion MRI predicts IDH mutation status and prognosis in high-grade gliomas. *Eur Radiol* 30:3254–3265. <https://doi.org/10.1007/s00330-020-06702-2>
 18. Barresi V, Eccher A, Simbolo M et al (2020) Diffuse gliomas in patients aged 55 years or over: a suggestion for IDH mutation testing. *Neuropathology* 40:68–74. <https://doi.org/10.1111/neup.12608>
 19. Robinson C, Kleinschmidt-DeMasters BK (2017) IDH1 -Mutation in diffuse gliomas in persons age 55 years and over. *J Neuropathol Exp Neurol* 76:nlw112. <https://doi.org/10.1093/jnen/nlw112>
 20. Kickingereder P, Isensee F, Tursunova I et al (2019) Automated quantitative tumour response assessment of MRI in neuro-oncology with artificial neural networks: a multicentre, retrospective study. *Lancet Oncol* 20:728–740. [https://doi.org/10.1016/S1470-2045\(19\)30098-1](https://doi.org/10.1016/S1470-2045(19)30098-1)
 21. Isensee F, Jaeger PF, Kohl SAA et al (2021) nnU-Net: a self-configuring method for deep learning-based biomedical image segmentation. *Nat Methods* 18:203–211. <https://doi.org/10.1038/s41592-020-01008-z>
 22. Zhang Y, Brady M, Smith S (2001) Segmentation of brain MR images through a hidden Markov random field model and the expectation-maximization algorithm. *IEEE Trans Med Imaging* 20:45–57. <https://doi.org/10.1109/42.906424>
 23. Benjamin DJ, Berger JO, Johannesson M et al (2017) Redefine statistical significance. *Nat Hum Behav* 2:6–10. <https://doi.org/10.1038/s41562-017-0189-z>
 24. Mandrekar JN (2010) Receiver operating characteristic curve in Diagnostic Test Assessment. *J Thorac Oncol* 5:1315–1316. <https://doi.org/10.1097/JTO.0b013e3181ec173d>
 25. Dubinski D, Won S-Y, Rauch M et al (2021) Association of Isocitrate Dehydrogenase (IDH) Status with Edema to tumor ratio and its correlation with Immune Infiltration in Glioblastoma. *Front Immunol* 12:627650. <https://doi.org/10.3389/fimmu.2021.627650>
 26. Brendle C, Klose U, Hempel J-M et al (2020) Association of dynamic susceptibility magnetic resonance imaging at initial tumor diagnosis with the prognosis of different molecular glioma subtypes. *Neurol Sci off J Ital Neurol Soc Ital Soc Clin Neurophysiol* 41:3625–3632. <https://doi.org/10.1007/s10072-020-04474-7>
 27. Hempel J-M, Schittenhelm J, Klose U et al (2019) In vivo molecular profiling of human Glioma: cross-sectional observational study using dynamic susceptibility contrast magnetic resonance perfusion imaging. *Clin Neuroradiol* 29:479–491. <https://doi.org/10.1007/s00062-018-0676-2>
 28. Xing Z, Zhang H, She D et al (2019) IDH genotypes differentiation in glioblastomas using DWI and DSC-PWI in the enhancing and peri-enhancing region. *Acta Radiol* 60:1663–1672. <https://doi.org/10.1177/0284185119842288>
 29. Álvarez-Torres M, del López-Cerdán M, Andreu A Z, et al (2023) Vascular differences between IDH- wildtype glioblastoma and astrocytoma IDH -mutant grade 4 at imaging and transcriptomic levels. <https://doi.org/10.1002/nbm.5004>. *NMR Biomed* e5004
 30. Suh CH, Kim HS, Jung SC et al (2018) 2-Hydroxyglutarate MR spectroscopy for prediction of isocitrate dehydrogenase mutant glioma: a systemic review and meta-analysis using individual patient data. *Neuro Oncol* 20:1573–1583. <https://doi.org/10.1093/neuonc/noy113>
 31. Majós C, Pons-Escoda A, Naval P et al (2023) Proton MR spectroscopy shows improved performance to segregate high-grade astrocytoma subgroups when defined with the new 2021 World Health Organization classification of central nervous system tumors. *Eur Radiol* 34:2174–2182. <https://doi.org/10.1007/s00330-023-10138-9>
 32. Kaufmann TJ, Smits M, Boxerman J et al (2020) Consensus recommendations for a standardized brain tumor imaging protocol for clinical trials in brain metastases. *Neuro Oncol* 22:757–772. <https://doi.org/10.1093/neuonc/noaa030>
 33. Barajas RF, Politi LS, Anzalone N et al (2021) Consensus recommendations for MRI and PET imaging of primary central nervous system lymphoma: guideline statement from the International Primary CNS Lymphoma Collaborative Group (IPCG). *Neuro Oncol* 23:1056–1071. <https://doi.org/10.1093/neuonc/noab020>
 34. Paulson ES, Schmainda KM (2008) Comparison of dynamic susceptibility-weighted contrast-enhanced MR methods: recommendations for measuring relative cerebral blood volume in brain tumors. *Radiology* 249:601–613. <https://doi.org/10.1148/radiol.2492071659>
 35. Cindil E, Sendur HN, Cerit MN et al (2021) Validation of combined use of DWI and percentage signal recovery-optimized protocol of DSC-MRI in differentiation of high-grade glioma,

- metastasis, and lymphoma. *Neuroradiology* 63:331–342. <https://doi.org/10.1007/s00234-020-02522-9>
36. Wang F, Zhou X, Chen R et al (2023) Improved performance of non-preloaded and high flip-angle dynamic susceptibility contrast perfusion-weighted imaging sequences in the presurgical differentiation of brain lymphoma and glioblastoma. *Eur Radiol*. <https://doi.org/10.1007/s00330-023-09917-1>
37. Mangla R, Kolar B, Zhu T et al (2011) Percentage signal recovery derived from MR dynamic susceptibility contrast imaging is useful to differentiate common enhancing malignant lesions of the brain. *Am J Neuroradiol* 32:1004–1010. <https://doi.org/10.3174/ajnr.A2441>
38. Pons-Escoda A, Garcia-Ruiz A, Naval-Baudin P et al (2020) Presurgical identification of primary central nervous system lymphoma with normalized time-intensity curve: a pilot study of a new method to analyze DSC-PWI. *Am J Neuroradiol* 41:1816–1824. <https://doi.org/10.3174/ajnr.A6761>
39. Pons-Escoda A, Garcia-Ruiz A, Garcia-Hidalgo C et al (2023) MR dynamic-susceptibility-contrast perfusion metrics in the presurgical discrimination of adult solitary intra-axial cerebellar tumors. *Eur Radiol*. <https://doi.org/10.1007/s00330-023-09892-7>
40. Pons-Escoda A, García-Ruiz A, Naval-Baudin P et al (2022) Diffuse large B-Cell Epstein-Barr virus-positive primary CNS lymphoma in Non-AIDS patients: high diagnostic accuracy of DSC Perfusion Metrics. *AJNR Am J Neuroradiol* 43:1567–1574. <https://doi.org/10.3174/ajnr.A7668>
41. Garcia-Ruiz A, Pons-Escoda A, Grussu F et al (2024) An accessible deep learning tool for voxel-wise classification of brain malignancies from perfusion MRI. *Cell Rep Med* 5:101464. <https://doi.org/10.1016/j.xcrm.2024.101464>
42. Cindil E, Sendur HN, Cerit MN et al (2022) Prediction of IDH Mutation Status in High-grade gliomas using DWI and high T1-weight DSC-MRI. *Acad Radiol* 29:S52–S62. <https://doi.org/10.1016/j.acra.2021.02.002>
43. Pons-Escoda A, Garcia-Ruiz A, Naval-Baudin P et al (2024) Differentiating IDH-mutant astrocytomas and 1p19q-codeleted oligodendrogliomas using DSC-PWI: high performance through cerebral blood volume and percentage of signal recovery percentiles. *Eur Radiol*. <https://doi.org/10.1007/s00330-024-10611-z>
44. Lee MD, Baird GL, Bell LC et al (2019) Utility of Percentage Signal Recovery and Baseline Signal in DSC-MRI optimized for relative CBV measurement for differentiating Glioblastoma, Lymphoma, Metastasis, and Meningioma. *Am J Neuroradiol* 40:1145–1450. <https://doi.org/10.3174/ajnr.A6153>

Publisher's Note Springer Nature remains neutral with regard to jurisdictional claims in published maps and institutional affiliations.